Stabilization of [WF$_5$]$^+$ by Bidentate N-Donor Ligands

Douglas Turnbull[a], Stacey D. Wetmore[a], Michael Gerken*[a]

Abstract: Transition-metal hexafluorides do not exhibit fluoride-ion donor properties in the absence of donor ligands. We report the first synthesis of donor-stabilized [MF$_5$]$^+$ derived from a transition-metal hexafluoride via fluoride-ion abstraction using WF$_6$(L) (L = 2,2'-bipy, 1,10-phen) and SbF$_5$(OSO) in SO$_2$. The [WF$_5$(L)][Sb$_2$F$_{11}$] salts and [WF$_5$(1,10-phen)][SbF$_6$]·SO$_2$ have been characterized by X-ray crystallography, Raman spectroscopy, and multinuclear NMR spectroscopy. The reaction of WF$_6$(2,2'-bipy) with an equimolar amount of SbF$_5$(OSO) reveals an equilibrium between [WF$_5$(2,2'-bipy)]$^+$ and the [WF$_4$(2,2'-bipy)$_2$]$^{2+}$ dication, as determined by ^{19}F NMR spectroscopy. The geometries of the cations in solid state are reproduced by gas-phase geometry optimizations (DFT-B3LYP), and NBO analyses reveal that the positive charges of the cations are stabilized primarily by compensatory σ-electron donation from the N-donor ligands.

The transition-metal hexafluorides (MF$_6$, M = Mo, W, Tc, and Re) behave as moderate-strength Lewis acids and F$^-$ acceptors, forming [MF$_7$]$^-$ and [MF$_8$]$^{2-}$ salts.[1–3] Conversely, they are not expected to behave as F$^-$ donors, which is exemplified by the use of WF$_6$ as an inert solvent for reactions between the strong acceptors SbF$_5$ and BiF$_5$.[4] Cationic derivatives of the transition-metal hexafluorides (i.e. [MF$_5$]$^+$) or fluorine-bridged, polarized species (i.e. F$_5$M–F---SbF$_5$), however, may play important roles in their chemistry. For instance, the oxidation of C$_6$F$_6$ by OsF$_6$ to afford [C$_6$F$_6$][Os$_2$F$_{11}$] is catalyzed by SbF$_5$,[5] and while the neat oxidation of xenon by IrF$_6$ to form [XeF][IrF$_6$] only occurs at an appreciable rate upon heating to 45 °C, the addition of SbF$_5$ allows for the low-temperature preparation of [XeF][IrSbF$_{11}$].[6]

There are few examples of cationic derivatives of transition-metal hexafluorides, which are prepared by the ligand-induced autoionization of WF$_6$ in the presence of bidentate Lewis bases (B') to form [WF$_4$(B')$_2$]$^{2+}$ salts.[7–9] Similar Lewis-acid behaviour towards bidentate Lewis bases is well documented for NbF$_5$ and TaF$_5$.[10,11] A monocationic derivative of a transition-metal hexafluoride, [MF$_5$]$^+$, or its donor-stabilized derivatives have not been previously reported. Herein, we report, to our knowledge, the first examples of such species in the form of [WF$_5$]$^+$ stabilized by the bidentate N-donor ligands 2,2'-bipyridine (2,2'-bipy) and 1,10-phenathroline (1,10-phen).

[a]   D. Turnbull, Prof. Dr. S. D. Wetmore, Prof. Dr. M. Gerken
Canadian Centre for Research in Advanced Fluorine Technologies
and Department of Chemistry and Biochemistry
University of Lethbridge
4401 University Drive
Lethbridge, AB
T1K 3M4
(Canada)
E-mail: michael.gerken@uleth.ca

Supporting information for this article is given via a link at the end of the document.

To access [WF$_5$(L)]$^+$ (L = 2,2'-bipy, 1,10-phen) salts, neutral, octacoordinate WF$_6$(L) adducts were employed as precursors, which were readily prepared by the reaction of WF$_6$(NC$_5$H$_5$) with L in CH$_2$Cl$_2$ (Eq. 1). The WF$_6$(2,2'-bipy) adduct has previously been prepared by the reaction of WF$_6$ with one molar equivalent of 2,2'-bipy,[8] and we have found that using a solid synthetic equivalent to gaseous WF$_6$ allows for more facile control of the stoichiometry. Due to the insolubility of WF$_6$(L) in compatible organic solvents and SO$_2$, the adducts were characterized by Raman spectroscopy in the solid state (Tables S6 and S7, Figures S11 and S12), and their structures were investigated by gas-phase geometry optimizations (Table S2), revealing distorted dodecahedral geometries (Figure 1).
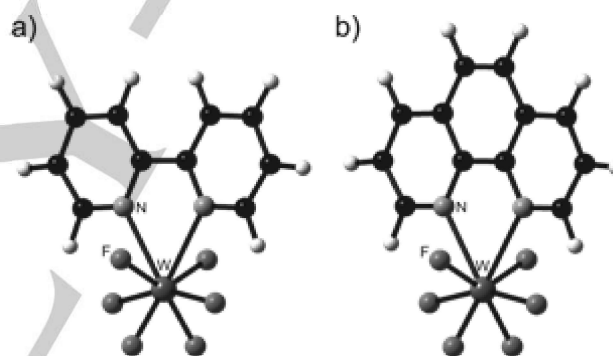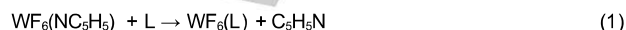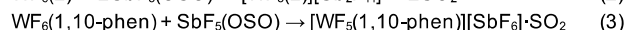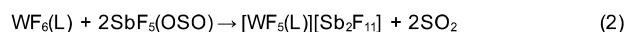
$$WF_6(NC_5H_5) + L \rightarrow WF_6(L) + C_5H_5N \qquad (1)$$

Figure 1. Optimized gas-phase structures of a) WF$_6$(2,2'-bipy) and b) WF$_6$(1,10-phen).

The WF$_6$(L) adducts react with two molar equivalents of SbF$_5$(OSO) in SO$_2$ at ambient temperature, yielding [WF$_5$(L)][Sb$_2$F$_{11}$] as yellow (L = 2,2'-bipy) or orange (L = 1,10-phen) solids upon removal of the volatile materials *in vacuo* (Eq. 2). Whereas the equimolar reaction of WF$_6$(1,10-phen) and SbF$_5$(OSO) in SO$_2$ yielded [WF$_5$(1,10-phen)][SbF$_6$]·SO$_2$ as an orange solid upon isolation (Eq. 3), the analogous reaction using WF$_6$(2,2'-bipy) was not found to afford a single, isolable product based on ^{19}F NMR spectroscopy in SO$_2$ (*vide infra*).

$$WF_6(L) + 2SbF_5(OSO) \rightarrow [WF_5(L)][Sb_2F_{11}] + 2SO_2 \qquad (2)$$
$$WF_6(1,10\text{-}phen) + SbF_5(OSO) \rightarrow [WF_5(1,10\text{-}phen)][SbF_6]\cdot SO_2 \qquad (3)$$

An incipient black material was observed in the incompletely reacted solid mixtures of WF$_6$(L) and SbF$_5$(OSO) after the introduction of solvent and warming to −70 °C. In the 1:1 reactions, this color disappeared immediately upon brief agitation at low temperature, but in the 1:2 reactions, it persisted in solution and dissipated over *ca.* 16 h at ambient temperature. The ^{19}F NMR spectrum of a freshly prepared solution of [WF$_5$(2,2'-bipy)][Sb$_2$F$_{11}$] revealed a small singlet at 235 ppm that disappeared in conjunction with the

Table 1. Selected Bond Lengths (Å) and Angles (°) of [WF$_5$(2,2'-bipy)]$^+$ and [WF$_5$(1,10-phen)]$^+$

	[WF$_5$(2,2'-bipy)]$^+$		[WF$_5$(1,10-phen)]$^+$		
	exptl	calcd[a]	exptl[b]	exptl[c]	calcd[a]
W–F(1)	1.854(3)	1.844	1.860(2)	1.861(3)	1.844
W–F(2)	1.842(3)	1.846	1.842(2)	1.844(3)	1.848
W–F(3)	1.842(3)	1.844	1.8377(19)	1.853(2)	1.843
W–F(4)	1.838(3)	1.846	1.852(2)	1.832(3)	1.848
W–F(5)	1.850(3)	1.850	1.8459(18)	1.856(2)	1.848
W–N(1)	2.234(4)	2.290	2.240(3)	2.223(4)	2.294
W–N(2)	2.224(4)	2.290	2.230(3)	2.229(3)	2.294
W···F(6)	3.085(4)		3.167(2)	3.244(3)	
F(1)–W–F(2)	77.56(15)	77.7	77.64(10)	77.95(12)	77.6
F(1)–W–F(3)	80.71(14)	82.7	80.54(9)	80.17(11)	83.2
F(1)–W–F(4)	78.14(15)	77.7	76.99(10)	78.52(12)	77.6
F(1)–W–F(5)	129.41(14)	126.9	128.78(9)	129.91(11)	125.9
F(1)–W–N(1)	136.61(16)	138.1	137.30(10)	133.24(12)	138.2
F(1)–W–N(2)	136.65(16)	79.8	136.14(10)	137.42(12)	80.2
N(1)–W–N(2)	71.53(15)	70.4	72.30(10)	72.45(13)	70.9

[a] Calculated using the B3LYP functional with the aug-cc-pVTZ-PP (W), aug-cc-pVTZ (N, F), and cc-pVTZ (H, C) basis sets. [b] From [WF$_5$(1,10-phen)][Sb$_2$F$_{11}$]. [c] From [WF$_5$(1,10-phen)][SbF$_6$]·SO$_2$.

loss of color, suggesting that its source could be an intermediate tungsten(VI) complex undergoing intense ligand-to-metal charge transfer (LCMT).

The geometries of the [WF$_5$(L)]$^+$ cations, as determined by X-ray crystallography, can be described as monocapped-octahedral, in which F(1) is capping and F(5), N(1), and N(2) form the trigonal base (Figure 2a). Alternatively, the geometries can, perhaps more accurately, be described as 4:3 polyhedra in which four fluorido ligands form the square face and F(3), N(1), and N(2) form the triangular face (Figures S8 and S9, Tables S4 and S5). Gas-phase geometry optimizations excellently reproduced the experimental geometries (Figure 2c), with only minor overestimations of the W–N bond lengths (Table 1). The crystal structures show weak W···F cation-anion contacts (3.085(4)–3.244(3) Å; Σ_r(vdW) = 1.47(F)[12] + 2.007(W)[13] = 3.48 Å). These contacts cap the square face of the 4:3 polyhedron (Figure 2b), resulting in a "monocapped 4:3" coordination sphere that does not otherwise conform to the archetypal octacoordinate geometries.[14]

While discrete ion pairs with zero net charge are found in [WF$_5$(2,2'-bipy)][Sb$_2$F$_{11}$] and [WF$_5$(1,10-phen)][SbF$_6$]·SO$_2$ (Figure S10), in [WF$_5$(1,10-phen)][Sb$_2$F$_{11}$], the ions aggregate to form [{WF$_5$(1,10-phen)}$_2$(μ-Sb$_2$F$_{11}$)]$^+$ units (Figure 3) with one equivalent of non-coordinated [Sb$_2$F$_{11}$]$^-$ acting as the counterion. The bridging anion adopts a pseudo-D_{4h}-symmetric geometry. Similar coordination motifs for fluoridoantimonate anions have been observed in crystallographic studies of Brønsted-superacidic systems; pseudo-D_{4h}-symmetric, bridging [Sb$_2$F$_{11}$]$^-$ anions were observed in [H$_3$F$_2$][Sb$_2$F$_{11}$][15] while [(CH$_3$)$_2$COH···SbF$_6$···HOC(CH$_3$)$_2$]$^+$ units were observed in [(CH$_3$)$_2$COH][SbF$_6$].[16]
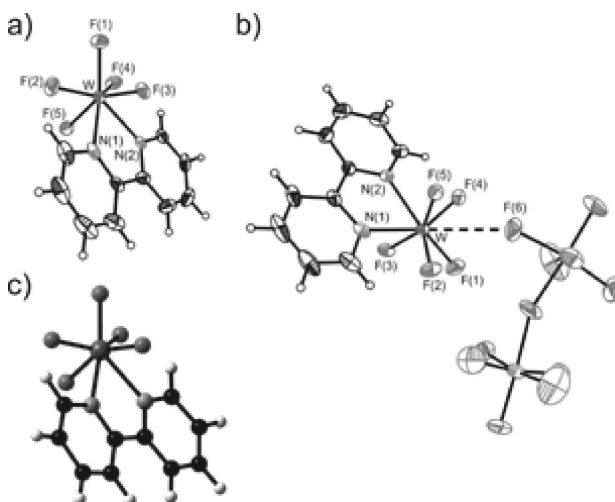

Figure 2. Thermal ellipsoid plots (50% probability level) of the a) cation and b) ion pair in [WF$_5$(2,2'-bipy)][Sb$_2$F$_{11}$], and c) the optimized gas-phase structure of [WF$_5$(2,2'-bipy)]$^+$.

The bonds and angles within the WF_5N_2 moieties differ only marginally, if at all, beyond experimental error (3σ) between the cations and any such differences are likely a consequence of crystal packing effects. The W–F bond lengths lie, on average (*ca*. 1.84 Å), between those of crystalline WF_6 (1.8261(13)–1.8266(19) Å)[17] and the known heptacoordinate WF_6 adducts (*ca*. 1.87 Å),[18] illustrating a compromise between increased Lewis acidity at the cationic tungsten centre and increased steric repulsion with respect to WF_6. Comparisons to $[WF_4(2,2'-bipy)_2]^{2+}$ (1.836(4) Å)[8] and $[WF_4(P_2Ar)_2]^{2+}$ (1.91(4)–1.93(4) Å; P_2Ar = 1,2-bis(dimethylphosphino)benzene) reveal no appreciable differences in W–F bond lengths,[9] though these bonds are significantly elongated in the arsenic analogue $[WF_4(As_2Ar)_2]^{2+}$ (2.114(6) Å).[9] The W–N bonds, meanwhile, are similar to those of $WF_6(NC_5H_5)$ and its derivatives (*ca*. 2.25 Å)[18] and $[WF_4(2,2'-bipy)_2]^{2+}$ (2.263(7) Å),[8] but much shorter than in $WF_6(NC_5H_5)_2$ (2.344(6) Å).[19] The calculated W–F (*ca*. 1.85 Å) and W–N (*ca*. 2.29 Å) bond lengths of $[WF_5(L)]^+$ are contracted with respect to those of the parent $WF_6(L)$ adducts (*ca*. 1.88 and 2.55 Å, respectively).
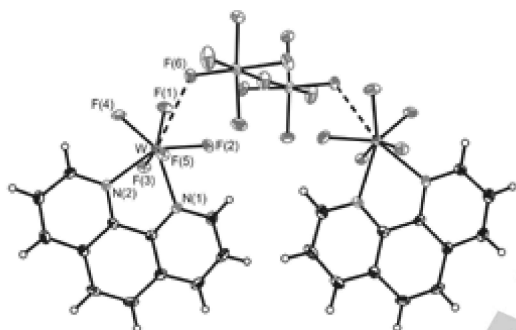

Figure 3. Thermal ellipsoid plot (50% probability level) of the $[\{WF_5(1,10-phen)\}_2(\mu-Sb_2F_{11})]^+$ unit in $[WF_5(1,10-phen)][Sb_2F_{11}]$.

From their Raman spectra (Figures S13–S15), the $\nu_s(WF_5)$ modes of $[WF_5(1,10-phen)][Sb_2F_{11}]$ (solid: 717/707 cm^{-1}), $[WF_5(1,10-phen)][SbF_6]\cdot SO_2$ (solid: 707 cm^{-1}), and $[WF_5(2,2'-bipy)][Sb_2F_{11}]$ (*ca*. 0.8 M solution in SO_2: 716 cm^{-1}) are consistent with known heptacoordinate fluoridotungsten(VI) complexes (*cf*. $WF_6(NC_5H_5)$ and $[WF_7]^-$: 705 cm^{-1}),[19,20] exhibiting a significant red-shift from free WF_6 (771 cm^{-1}).[21] The splitting of the $\nu_s(WF_5)$ mode in $[WF_5(1,10-phen)][Sb_2F_{11}]$ is attributed to vibrational coupling of the two WF_5 moieties within the $[\{WF_5(1,10-phen)\}_2(\mu-Sb_2F_{11})]^+$ unit. In all cases, bands corresponding to the nitrogen bases tend to be blue-shifted. See the Supporting Information for further details.

The ^{19}F NMR spectra of $[WF_5(L)][Sb_2F_{11}]$ and $[WF_5(1,10-phen)][SbF_6]$ in SO_2 are comprised of broad singlets at 206 (L = 2,2'-bipy; $\Delta\nu_{1/2}$ = 15 Hz) and 204 ppm (L = 1,10-phen; $\Delta\nu_{1/2}$ = 140 Hz). These are much higher in frequency than free WF_6 (167 ppm), consistent with highly electron-poor tungsten centers and a fluxional coordination environment. Cooling to −70 °C was not sufficient to suppress exchange, though $[WF_5(1,10-phen)]^+$ was observed to reach the coalescence point (Figure 4).

The fluorine-on-tungsten regions in the ^{19}F NMR spectra of *ca*. 1:1 mixtures of $WF_6(2,2'-bipy)$ and $SbF_5(OSO)$ in SO_2 consist of varying proportions of $[WF_5(2,2'-bipy)]^+$, WF_6, and $[WF_4(2,2'-bipy)_2]^{2+}$ (Eq. 4). It is observed that if $SbF_5(OSO)$ is present in a slight excess (1.0:1.1), the monocation is better stabilized, whereas if the ratio of reactants is closer to equimolar, a greater degree of decomposition to the dication and WF_6 is observed (see the Supporting Information). While a suspension of sparingly soluble $[WF_5(1,10-phen)][SbF_6]\cdot SO_2$

in SO_2 reveals only small amounts of $[WF_4(1,10-phen)_2]^{2+}$ and WF_6 at ambient temperature, heating to 45 °C results in increased proportions of the dismutation products. This indicates that the dismutation of $[WF_5(2,2'-bipy)]^+$ is facilitated by the lability of 2,2'-bipy via rotation about the C–C' bond, and that $[WF_5(1,10-phen)]^+$ is kinetically stabilized by the increased rigidity of 1,10-phen.

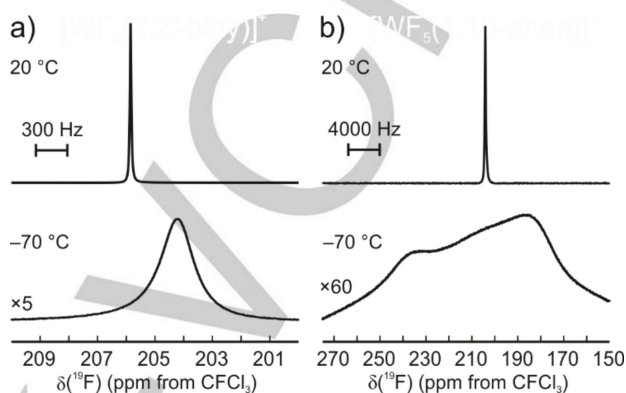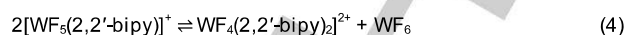$$2[WF_5(2,2'-bipy)]^+ \rightleftharpoons WF_4(2,2'-bipy)_2]^{2+} + WF_6 \qquad (4)$$

Figure 4. Fluorine-on-tungsten resonances in the ^{19}F NMR spectra of a) $[WF_5(2,2'-bipy)][Sb_2F_{11}]$ and b) $[WF_5(1,10-phen)][Sb_2F_{11}]$ in SO_2 at 20 and −70 °C.

As such, we postulate that $[WF_5(B')]^+$ is formed as an intermediate in the ligand-induced autoionization of WF_6, but is destabilized by the relatively fluorobasic $[WF_7]^-$ anion, resulting in quantitative conversion to $[WF_4(B')_2]^{2+}$. Substitution of $[WF_7]^-$ with $[SbF_6]^-$ is sufficient to achieve a stable equilibrium between the mono- and dications, whereas $[Sb_2F_{11}]^-$ is required to fully stabilize the monocation.

Molecular-orbital calculations reveal that the HOMO-LUMO transitions of $WF_6(L)$, $[WF_5(L)]^+$, and $[WF_4(2,2'-bipy)_2]^{2+}$ are LMCT in nature (Figure 5, Table S10). The frontier MOs of free, trigonal-bipyramidal $[WF_5]^+$, the structure of which has been optimized for the purposes of comparison (Figure S7), consist of $\pi(d_{x(y)z}(W)-p_{x(y)}(F))$ interactions that are net antibonding in nature (Figure S19). The relative LUMO energies (Table 2) indicate that while $WF_6(L)$ are weaker oxidizing agents than free WF_6, the cations are significantly stronger.

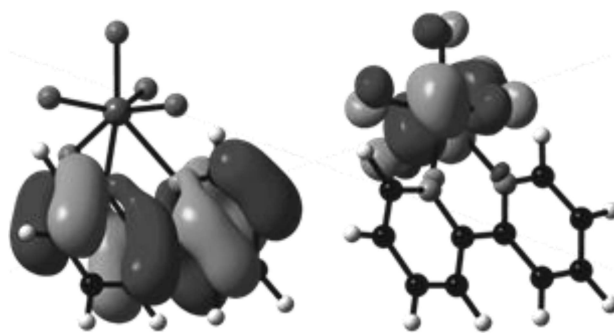Figure 5. Frontier molecular orbitals of $[WF_5(2,2'-bipy)]^+$: HOMO (left) and LUMO (right). Isosurface values are drawn at 0.04 e Å^{-3}.

Natural-bond-orbital (NBO) analyses reveal that upon F^- abstraction from $WF_6(L)$ to form $[WF_5(L)]^+$, a slight increase in the energies is observed for $\pi(lp(F) \rightarrow lv(W))$ (lp = lone pair, lv = lone valence) interactions (Tables S13 and S14). More so, there is a substantial increase in the total $\sigma(lp(N) \rightarrow lv(W))$ interaction energies, indicating that the positive charge introduced to the tungsten center is stabilized by compensatory electron donation from the surrounding ligands, especially the N-donor ligands. This is paralleled by the natural-population-analysis (NPA) charges on tungsten hardly increasing upon F^- abstraction from $WF_6(L)$ (+2.57) to $[WF_5(L)]^+$ (+2.59), and even decreasing to $[WF_4(2,2'\text{-bipy})_2]^{2+}$ (+2.39), for which the $\sigma(lp(N) \rightarrow lv(W))$ interactions are strongest. Correspondingly, the NPA charges residing on the ligands increase in the order of $WF_6(L)$ < $[WF_5(L)]^+$ < $[WF_4(2,2'\text{-bipy})_2]^{2+}$ (Table 2). Furthermore, there is a significant increase in the average Wiberg bond indices (WBIs) from $WF_6(L)$ to $[WF_5(L)]^+$ in the polar-covalent W–F (0.72 → 0.80) and dative W–N (0.27 → 0.42) bonds. Whereas the W–N bonds in $WF_6(L)$ are predicted to be approximately one-third the order of the W–F bond, this proportion increases to more than one half in the cations. To contrast, the absence of N-donor ligands in the hypothetical $[WF_5]^+$ cation results in highly covalent W–F bonds (F_{eq}: 0.95; F_{ax}: 0.90) and a highly positively charged tungsten centre (+2.82).

In conclusion, $[WF_5(L)]^+$ cations have been stabilized by the N-donor ligands 2,2'-bipy and 1,10-phen, resulting in the first isolated complexes of transition-metal $[MF_5]^+$ cations. The $[WF_5(L)]^+$ cations have been found to adopt distorted monocapped-octahedral or, alternatively, 4:3 geometries in the solid state, though in solution these geometries are fluxional on the NMR timescale. Fluorine-19 NMR studies revealed the thermodynamic instability of the $[SbF_6]^-$ salts and implicate heptacoordinate $[WF_5]^+$ derivatives as reactive intermediates in the ligand-induced autoionization of WF_6. The positive charges of the cations are stabilized primarily by increased σ-electron donation from the N-donor ligands.

Table 2. Selected MO Energies (eV), NPA Charges, and WBIs of Various Fluoridotungsten(VI) Complexes[a]

	E_{LUMO}	Charge		WBI	
		W	L	W–F	W–N
WF_6	−4.83	+2.69		0.80	
$[WF_5]^+$ (D_{3h})	−11.20	+2.82		0.90–0.95	
$[WF_5]^+$ (C_{4v})	−11.18	+2.83		0.92–0.98	
$WF_6(NC_5H_5)_2$	−2.81	+2.58	+0.44[b]	0.69–0.72	0.32
$WF_6(2,2'\text{-bipy})$	−2.96	+2.57	+0.38	0.71–0.74	0.27
$WF_6(1,10\text{-phen})$	−2.94	+2.57	+0.39	0.71–0.74	0.27
$[WF_5(2,2'\text{-bipy})]^+$	−7.50	+2.59	+0.62	0.79–0.82	0.42
$[WF_5(1,10\text{-phen})]^+$	−7.43	+2.59	+0.62	0.79–0.83	0.42
$[WF_4(2,2'\text{-bipy})_2]^{2+}$	−10.02	+2.39	+0.71[c]	0.76	0.46

[a] Calculated using the B3LYP functional with the aug-cc-pVTZ-PP (W), aug-cc-pVTZ (N, F), and cc-pVTZ (H, C) basis sets. [b] For both pyridyl ligands combined. [c] For each 2,2'-bipy ligand.

Conflict of Interest

The authors declare no conflict of interest.

Keywords: Fluorine • Lewis acids • Cations • Heptacoordinate complexes • X-ray crystallography

[1]   R. Craciun, R. T. Long, D. A. Dixon, K. O. Christe, *J. Phys. Chem. A* **2010**, *114*, 7571–7582.
[2]   R. Craciun, D. Picone, R. T. Long, S. Li, D. A. Dixon, K. A. Peterson, K. O. Christe, *Inorg. Chem.* **2010**, *49*, 1056–1070.
[3]   M. J. Molski, K. Seppelt, *Dalton Trans.* **2009**, 3379.
[4]   G. S. H. Chen, J. Passmore, P. Taylor, T. K. Whidden, *Inorg. Nucl. Chem. Lett.* **1976**, *12*, 943–948.
[5]   H. Shorafa, D. Mollenhauer, B. Paulus, K. Seppelt, *Angew. Chem. Int. Ed.* **2009**, *48*, 5845–5847.
[6]   F. Tamadon, S. Seidel, K. Seppelt, *Acta Chim. Slov.* **2013**, *60*, 491–494.
[7]   L. Arnaudet, R. Bougon, B. Ban, M. Lance, A. Navaza, M. Nierlich, J. Vigner, *J. Fluorine Chem.* **1992**, *59*, 141–152.
[8]   L. Arnaudet, R. Bougon, B. Ban, M. Lance, A. Navaza, M. Nierlich, J. Vigner, *J. Fluorine Chem.* **1994**, *67*, 17–25.
[9]   W. Levason, F. M. Monzittu, G. Reid, W. Zhang, *Chem. Commun.* **2018**, *54*, 11681–11684.
[10]   F. Marchetti, G. Pampaloni, *Chem. Commun.* **2012**, *48*, 635–653.
[11]   S. L. Benjamin, W. Levason, G. Reid, *Chem. Soc. Rev.* **2013**, *42*, 1460–1499.
[12]   A. Bondi, *J. Phys. Chem.* **1964**, *68*, 441–451.
[13]   S. S. Batsanov, *J. Mol. Struct.* **1999**, *468*, 151–159.
[14]   M. G. B. Drew, *Coord. Chem. Rev.* **1977**, *24*, 179–275.
[15]   D. Mootz, K. Bartmann, *Angew. Chem. Int. Ed. Engl.* **1988**, *27*, 391–392.
[16]   D. Stuart, S. D. Wetmore, M. Gerken, *Angew. Chem. Int. Ed.* **2017**, *56*, 16380–16384.
[17]   T. Drews, J. Supel, A. and Hagenbach, K. Seppelt, *Inorg. Chem.* **2006**, *45*, 3782–3788.
[18]   D. Turnbull, N. Kostiuk, S. D. Wetmore, M. Gerken, *J. Fluorine Chem.* **2018**, *215*, 1–9.
[19]   L. Arnaudet, R. Bougon, B. Buu, M. Lance, M. Nierlich, P. Thuéry, J. Vigner, *J. Fluorine Chem.* **1995**, *71*, 123–129.
[20]   A. Beuter, W. Kuhlmann, W. Sawodny, *J. Fluorine Chem.* **1975**, *6*, 367–378.
[21]   H. H. Claassen, H. Selig, *Isr. J. Chem.* **1969**, *7*, 499–504.

Entry for the Table of Contents

COMMUNICATION

The Lewis acidity of WF_6 towards nitrogen bases has been exploited to isolate the first donor-stabilized $[MF_5]^+$ cations derived from a transition-metal hexafluoride. The $[WF_5(L)]^+$ (L = 2,2'-bipyridine, 1,10-phenanthroline) cations have been isolated as stable $[Sb_2F_{11}]^-$ salts and found to adopt monocapped-octahedral or 4:3 geometries in the solid state. Cations of this type are implicated as unstable intermediates in the ligand-induced autoionization of WF_6.
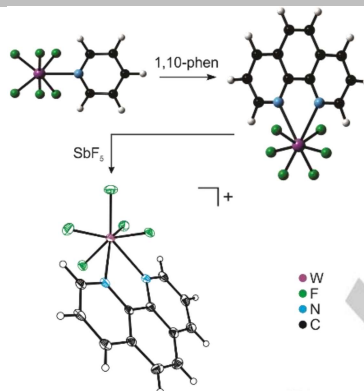
Douglas Turnbull, Stacey D. Wetmore, Michael Gerken*

Page No. – Page No.

Stabilization of $[WF_5]^+$ by Bidentate N-Donor Ligands

COMMUNICATION

((Insert TOC Graphic here))

Author(s), Corresponding Author(s)*

Page No. – Page No.

Title

Text for Table of Contents